Robust Hovering Control of a Quad Tilt-Wing UAV

C. Hancer, K. T. Oner, E. Sirimoglu, E. Cetinsoy, M. Unel
Sabanci University, Orhanli-Tuzla 34956, Istanbul TURKEY
e-mail: {chancer,kaanoner,efesirimoglu,cetinsoy,munel}@sabanciuniv.edu

***Abstract*—This paper presents design of a robust hovering controller for a quad tilt-wing UAV to hover at a desired position under external wind and aerodynamic disturbances. Wind and the aerodynamic disturbances are modeled using the Dryden model. In order to increase the robustness of the system, a disturbance observer is utilized to estimate the unknown disturbances acting on the system. Nonlinear terms which appear in the dynamics of the vehicle are also treated as disturbances and included in the total disturbance. Proper compensation of disturbances implies a linear model with nominal parameters. Thus, for robust hovering control, only PID type simple controllers have been employed and their performances have been found very satisfactory. Proposed hovering controller has been verified with several simulations and experiments.**

I. Introduction

There have been remarkable advances in the design and development of autonomous unmanned aerial vehicles (UAV) in recent years. Quadrotors are relatively more stable platforms than helicopters. One of the basic tasks for an autonomously flying quadrotor/helicopter is to hover at a given point in space and maintain that position despite the external disturbances.

For position hold Hoffmann et al. [1] use thrust vectoring with PID structure. The position hold performance in x-y plane is within an error of 40 cm radius whereas altitude control error is within 30 cm, verified by experiments. In the work of Meister et al. [2], a sensor fusion algorithm for stable attitude and position estimation using GPS, IMU and compass modules together, is presented, and the control algorithms for position hold and waypoint tracking are developed. It is reported that the position hold error under a wind disturbance less than 5 m/s is bounded by 3 m. Hoffmann et al. [3] develop an autonomous trajectory tracking algorithm through cluttered environments for the STARMAC platform and a novel algorithm for dynamic trajectory generation. Both indoor and outdoor flight tests are performed, and an indoor accuracy of 10 cm and an outdoor accuracy of 50 cm are reported. Puls et al. [4] presents the development of a position control system based on 2D GPS data for quadrotor vehicles. Using the proposed algorithm, the vehicle is able to keep positions above given destinations as well as to navigate between waypoints while minimizing trajectory errors. Waslander and Wang [5] focus on improvement of STARMAC quadrotor position hold performance by modeling the wind effects, i.e. using Dryden Wind Gust Model, on quadrotor dynamics in order to estimate wind velocities during fight. The performance of the controller and the disturbance rejection is evaluated only in simulations.

Soundararaj et al. [6] proposes purely vision based position control using only an onboard light weight camera. The satisfactory performance of this approach in hovering and following the user defined trajectories is validated by flight tests. In the work of Azrad et al. [7], an object tracking system using an autonomous Micro Air Vehicle (MAV) is described. Experimental results obtained from outdoor flight tests showed that the vision-control system enabled the MAV to track and hover above the target as long as the battery is available.

In this work, we develop a robust hovering control system for the quad tilt-wing aerial vehicle SUAVI (Sabanci University Unmanned Aerial VehIcle) (see Figure 1). Dryden model is used to model wind gusts acting on the vehicle and these disturbances are included in the dynamic model of the vehicle. Thus, aerodynamic disturbances, which are not considered in many studies, are integrated into the system model. In order to estimate and compensate for the unknown disturbances, a "disturbance observer" [8] is utilized. This observer also takes into account the nonlinear terms in the dynamics of the vehicle and treats them as disturbances. As a result, a linear dynamical model with nominal parameters has been obtained. PID type controllers are employed to achieve robust hovering. The proposed observer based control approach is verified by simulations and experiments, and its performance has been found quite satisfactory.

Organization of the paper is as follows: Section II introduces the mathematical model of the vehicle including wind effects. Section III describes the design of the disturbance observer. Section IV is on flight controllers where hovering and attitude controllers are designed. Section V and VI are on simulation and experimental results, and related discussions. Finally, Section VII concludes the paper with some remarks and indicates possible future directions.

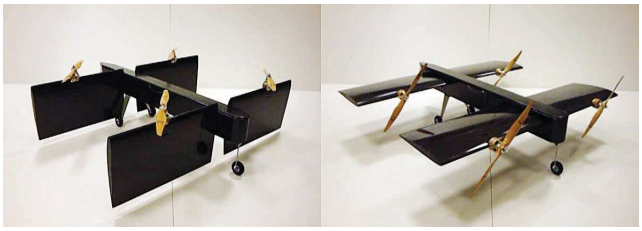

Fig. 1. SUAVI in different flight configurations

II. Dynamical Model of the Vehicle

In deriving dynamical models for unmanned aerial vehicles, it is usually preferred to express positional dynamics with respect to a fixed world coordinate frame and the rotational

978-1-4244-5226-2/10/$26.00 ©2010 IEEE

dynamics with respect to a body fixed frame attached to the vehicle. Making rigid body assumption, the dynamics of an unmanned aerial vehicle can be written as

$$\begin{bmatrix} mI_{3x3} & 0_{3x3} \\ 0_{3x3} & I_b \end{bmatrix} \begin{bmatrix} \dot{V}_w \\ \dot{\Omega}_b \end{bmatrix} + \begin{bmatrix} 0 \\ \Omega_b \times (I_b \Omega_b) \end{bmatrix} = \begin{bmatrix} F_t \\ M_t \end{bmatrix} \tag{1}$$

The subscripts w and b used in these equations express the vector and matrix quantities in world and body frames, respectively. V_w and Ω_b vectors represent the linear and the angular velocities of the vehicle with respect to the world and the body frames. m is the mass and I_b is the inertia matrix of the vehicle expressed in its body coordinate frame. I_{3x3} and 0_{3x3} matrices are 3×3 identity and zero matrices. Since the aerial vehicle is modeled as a 6 DOF rigid body, the left hand side of Equation (1) is standard for many aerial vehicles. Note that the total force and the moment, F_t and M_t, are platform dependent. We should remark that for a tilt-wing quadrotor these terms will be functions of the thrusts produced by the rotors and cosine and/or sine of the rotation angles of the wings (see [9] for details). Using vector-matrix notation above equations can be rewritten in a more compact form as

$$M\dot{\zeta} + C(\zeta)\zeta = G + O(\zeta)\omega + E(\xi)\omega^2 + W(\zeta) \tag{2}$$

where ζ denotes the vehicle's generalized velocity vector and is defined as

$$\zeta = [\dot{X}, \dot{Y}, \dot{Z}, p, q, r]^T \tag{3}$$

In (3), X, Y and Z are position coordinates of the center of mass of the vehicle with respect to the world frame, and p, q and r are angular velocities expressed in the body fixed frame. The vector ξ which appears in Equation (2), describes the position and the orientation of the vehicle with respect to the world frame, and is defined as

$$\xi = [X, Y, Z, \phi, \theta, \psi]^T \tag{4}$$

The mass-inertia matrix, M, the Coriolis-centripetal matrix, $C(\zeta)$, the gravity term, G, and the gyroscopic term are defined as

$$M = \begin{bmatrix} mI_{3x3} & 0_{3x3} \\ 0_{3x3} & diag(I_{xx}, I_{yy}, I_{zz}) \end{bmatrix} \tag{5}$$

$$C(\zeta) = \begin{bmatrix} 0 & 0 & 0 & 0 & 0 & 0 \\ 0 & 0 & 0 & 0 & 0 & 0 \\ 0 & 0 & 0 & 0 & 0 & 0 \\ 0 & 0 & 0 & 0 & I_{zz}r & -I_{yy}q \\ 0 & 0 & 0 & -I_{zz}r & 0 & I_{xx}p \\ 0 & 0 & 0 & I_{yy}q & -I_{xx}p & 0 \end{bmatrix} \tag{6}$$

$$G = [0, 0, mg, 0, 0, 0]^T \tag{7}$$

$$O(\zeta)\omega = J_{prop} \begin{pmatrix} 0_{3\times 1} \\ \sum_{i=1}^{4} J[\eta_i \Omega_b \times \begin{bmatrix} c_{\theta_i} \\ 0 \\ -s_{\theta_i} \end{bmatrix} \omega_i] \end{pmatrix} \tag{8}$$

where J_{prop} is the moment of inertia of the propeller about its rotation axis, $0_{3\times 1}$ is a 3×1 zero vector and ω_i is the propellers' speed.

System actuator vector, $E(\xi)\omega^2$, is defined as

$$E(\xi)\omega^2 = \begin{bmatrix} (c_\phi s_\theta c_\psi + s_\phi s_\psi)u_v + c_\psi c_\theta u_h \\ (c_\phi s_\theta s_\psi - s_\phi c_\psi)u_v + s_\psi c_\theta u_h \\ c_\phi c_\theta u_v - s_\theta u_h \\ (l_s s_{\theta_f} - c_{\theta_f}\lambda)u_{f_{dif}} + (l_s s_{\theta_r} + c_{\theta_r}\lambda)u_{r_{dif}} \\ (s_{\theta_f} u_{f_{sum}} - s_{\theta_r} u_{r_{sum}})l_l \\ (l_s c_{\theta_f} + s_{\theta_f}\lambda)u_{f_{dif}} + (l_s c_{\theta_r} - s_{\theta_r}\lambda)u_{r_{dif}} \end{bmatrix} \tag{9}$$

$u_{(h,v,f_{dif},r_{dif},f_{sum},r_{sum})}$ terms used in Equation (9) are the horizontal, vertical, front differential, rear differential, front sum and rear sum thrust forces, respectively and they are defined as

$$u_{f_{sum}} = k(\omega_1^2 + \omega_2^2),\ u_{r_{sum}} = k(\omega_3^2 + \omega_4^2) \tag{10}$$

$$u_{f_{dif}} = k(\omega_1^2 - \omega_2^2),\ u_{r_{dif}} = k(\omega_3^2 - \omega_4^2) \tag{11}$$

$$u_v = -s_{\theta_f} u_{f_{sum}} - s_{\theta_r} u_{r_{sum}},\ u_h = c_{\theta_f} u_{f_{sum}} + c_{\theta_r} u_{r_{sum}} \tag{12}$$

where the following constraints are imposed on the wing angles, namely

$$\theta_f = \theta_1 = \theta_2,\ \theta_r = \theta_3 = \theta_4 \tag{13}$$

Parameters l_s and l_l denote distances between the rotors and the center of mass of the vehicle, and the parameters k and λ are lift and drag coefficients, respectively.

Lift and drag forces produced by the wings and the resulting moments due to these forces for different wing angles are defined as

$$W(\zeta) = \begin{bmatrix} R_{wb} \begin{bmatrix} F_D^1 + F_D^2 + F_D^3 + F_D^4 \\ 0 \\ F_L^1 + F_L^2 + F_L^3 + F_L^4 \end{bmatrix} \\ l_s(F_L^1 - F_L^2 + F_L^3 - F_L^4) \\ l_l(F_L^1 + F_L^2 - F_L^3 - F_L^4) \\ l_s(-F_D^1 + F_D^2 - F_D^3 + F_D^4) \end{bmatrix} \tag{14}$$

where R_{wb} is the rotation matrix between world and body coordinate axis, $F_D^i = F_D^i(\theta_i, v_x, v_z)$ and $F_L^i = F_L^i(\theta_i, v_x, v_z)$ are the lift and drag forces produced at the wings.

We should remark that above model boils down to a quadrotor model when $(\theta_{1,2,3,4} = \pi/2)$.

A. Modeling Wind Gusts

In order to improve the positioning performance of the quadrotor, wind effects can be modeled and the generalized wind forces can be estimated. The wind estimate is used to reject the external disturbances created by the wind and gust effects.

The main framework of wind modeling represented in [6] depends on the Dryden wind-gust model. This model is defined as a summation of sinusoidal excitations:

$$v_\omega(t) = v_\omega^0 + \sum_{i=1}^{n} a_i sin(\Omega_i t + \varphi_i) \tag{15}$$

where $v_\omega(t)$ is a time dependent estimate of the wind vector given time t, randomly selected frequencies Ω_i in the range of 0.1 to 1.5 rad/s and phase shifts φ_i. n is the number of sinusoids, a_i is the amplitude of sinusoids and v_ω^0 is

the static wind vector. The magnitudes a_i are defined as $a_i = \sqrt{\Delta\Omega_i \Phi(\Omega_i)}$ where $\Delta\Omega_i$ are frequency intervals between different frequencies and $\Phi(\Omega_i)$ are the power spectral densities. The power spectral density for vertical and horizontal winds are different and can be determined from the following equations:

$$\Phi_h(\Omega) = \sigma_h^2 \frac{2L_h}{\pi} \frac{1}{1+(L_h\Omega)^2} \tag{16}$$

$$\Phi_v(\Omega) = \sigma_v^2 \frac{2L_v}{\pi} \frac{1+3(L_v\Omega)^2}{(1+(L_v\Omega)^2)^2} \tag{17}$$

Here σ_h and σ_v are horizontal and vertical turbulence intensities respectively. L_h and L_v are horizontal and vertical gust length scales. It is stated that these relations are valid for altitudes below 1000 feet [6]. The relations between L_h and L_v, and σ_h and σ_v are altitude dependent as can be seen from the following equations:

$$\frac{L_h}{L_v} = \frac{1}{(0.177+0.000823Z)^{1.2}} \tag{18}$$

$$\frac{\sigma_h}{\sigma_v} = \frac{1}{(0.177+0.000823Z)^{0.4}} \tag{19}$$

Using velocities predicted by this wind model, generalized forces are calculated by multiplying wind velocities by related aerodynamic drag coefficients. These generalized forces are integrated into the dynamic model given in Eq. (2) as external disturbances $D(\zeta,\xi)$. After incorporating the external disturbances, the final form of the dynamic model of the quadrotor vehicle given in Eq. (20) becomes as follows:

$$M\dot{\zeta} + C(\zeta)\zeta = G + O(\zeta)\omega + E(\xi)\omega^2 + W(\zeta) + D(\zeta,\xi) \tag{20}$$

III. Disturbance Observer

In this section, we design a disturbance observer [8] to estimate the total disturbance, i.e. external disturbances, nonlinear terms and parametric uncertainties, acting on the system.

We first note that the mass-inertia matrix of the aerial vehicle can be written as $M = M_{nom} + \tilde{M}$. Here, M_{nom} refers to the nominal inertia matrix with nominal mass and inertia parameters, and $(\tilde{M})$ is the difference between actual and nominal mass-inertia matrices.

Equation (20) can be rewritten in terms of the nominal inertia matrix explicitly as

$$M_{nom}\dot{\zeta} = f + \tau_{dist} \tag{21}$$

where f and τ_{dist} are the actuator input and and the total disturbance, respectively, and are defined as

$$f = E(\xi)\omega^2$$

$$\tau_{dist} = -\tilde{M}\dot{\zeta} - C(\zeta)\zeta + G + O(\zeta)\Omega + W(\zeta) + D(\zeta,\xi) \tag{22}$$

Note that τ_{dist} contains, in addition to the external disturbances like wind and gust, the nonlinear terms and the parametric uncertainties in the dynamics.

Equation (21) can be rewritten as 6 scalar equations of the form

$$M_{nom_i}\dot{\zeta}_i = f_i + \tau_{dist_i}, \quad i = 1,\ldots,6 \tag{23}$$

Taking the Laplace transform and solving for τ_{dist_i} imply

$$\tau_{dist_i}(s) = M_{nom_i} s\zeta_i(s) - f_i(s) \tag{24}$$

In order to estimate the disturbance given by (24), both sides of the equation can be multiplied by $G(s) = \frac{g}{s+g}$, i.e. transfer function of a low-pass filter, to obtain

$$G(s)\tau_{dist_i}(s) = M_{nom_i} sG(s)\zeta_i(s) - G(s)f_i(s) \tag{25}$$

Note that, $sG(s)$ can be written as

$$sG(s) = s\frac{g}{s+g} = g(1-\frac{g}{s+g}) = g(1-G(s)) \tag{26}$$

Let's define the term $G(s)\tau_{dist_i}(s)$ by $\hat{\tau}_{dist_i}(s)$, i.e. estimated disturbance. Thus,

$$\hat{\tau}_{dist_i}(s) = -G(s)f_i(s) - gM_{nom_i}G(s)\zeta_i(s) + gM_{nom_i}\zeta_i(s) \tag{27}$$

Subtracting the estimated disturbance from the control input, i.e. $f_i \leftarrow f_i - \hat{\tau}_{dist_i}$, we obtain

$$M_{nom_i} s\zeta_i(s) = f_i(s) + (1-G(s))\tau_{dist_i}(s) \tag{28}$$

Note that due to low-pass filter $G(s) \approx 1$ in the low frequency range. Thus, for low frequencies the total disturbance on the system is eliminated and the input-output description of the system becomes a linear model with nominal parameters, namely

$$M_{nom_i}\dot{\zeta}_i = f_i \tag{29}$$

The block diagram of the implemented disturbance observer is depicted in 2.

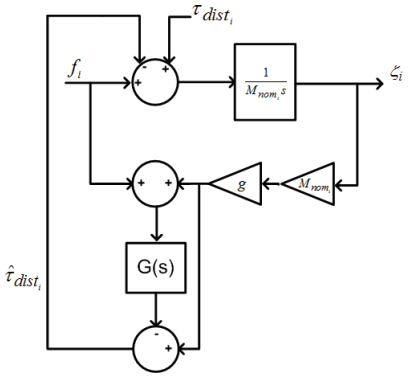

Fig. 2. Block diagram of the disturbance observer

IV. Flight Controllers

A. Hovering Controller

Suppose the aerial vehicle is in the VTOL (Vertical Take-Off and Landing) mode and the reference position and the desired altitude are defined as $\mathbf{x}^d$, z^d. It is aimed that the vehicle should not lose the reference position until reaching the desired altitude from the take-off position and then stay in the vicinity of the reference position at the desired altitude.

Let $\mathbf{x}_n$ ve $\mathbf{y}_n$ be the unit vectors along the x and y axes of the world frame, respectively. Let $x(t)$ denote instantaneous position of the vehicle provided by the GPS or the camera

and let e_x and e_y denote vehicle's position errors along x and y axes. Similar to the work in [3], we can write the following equations:

$$e_x = (\mathbf{x}^d - \mathbf{x}(t)) \cdot \mathbf{x}_n \tag{30}$$

$$\dot{e}_x = -\mathbf{v}(t) \cdot \mathbf{x}_n \tag{31}$$

$$e_y = (\mathbf{x}^d - \mathbf{x}(t)) \cdot \mathbf{y}_n \tag{32}$$

$$\dot{e}_y = -\mathbf{v}(t) \cdot \mathbf{y}_n \tag{33}$$

In order to hover the vehicle at a given position, PID controllers are designed along both x and y axes, namely

$$u_x = K_{x,p} e_x + K_{x,d} \dot{e}_x + K_{x,i} \int_0^t e_x dt \tag{34}$$

$$u_y = K_{y,p} e_y + K_{y,d} \dot{e}_y + K_{y,i} \int_0^t e_y dt \tag{35}$$

Note that these controllers are nothing else than the acceleration controllers along x and y axes. Depending on the heading, ψ, of the vehicle, these accelerations must be transformed using a 2D rotation matrix, $R(\psi)$, as follows:

$$a_{xy} = R(\psi)(u_x \cdot \mathbf{x_n} + u_y \cdot \mathbf{y_n}) \tag{36}$$

By using equation (36), reference attitude angles which allows the vehicle to hover at a given position can easily be computed using the following formulas:

$$\theta_{ref} = -\arcsin(\frac{a_x}{||a||}) \tag{37}$$

$$\phi_{ref} = \arcsin(\frac{a_y}{||a||\cos(\theta)}) \tag{38}$$

where a is the total acceleration of the vehicle, $a = (a_x, a_y, a_z)$, a_x and a_y are the x and y components of the acceleration vector, a_{xy}, defined by equation (36). The third component of the acceleration vector, a_z, is the acceleration of the vehicle along the z axis and is computed as $a_z = u_1/m$. $||a||$ is the Euclidean norm of a and is defined as

$$||a|| = \sqrt{a_x^2 + a_y^2 + a_z^2} \tag{39}$$

Reference attitude angles computed by (37) and (38) should be filtered through a low-pass filter to be used by the attitude controller introduced next.

B. Altitude and Attitude Controllers

In order to develop altitude and attitude controllers, we first recall the quadrotor's altitude and attitude dynamics; i.e.

$$\begin{aligned}
\ddot{Z} &= -c_\theta c_\phi \frac{u_1}{m} + g \\
\dot{p} &= \frac{u_2}{I_{xx}} + \frac{I_{yy} - I_{zz}}{I_{xx}} qr - \frac{J}{I_{xx}} q\omega_p \\
\dot{q} &= \frac{u_3}{I_{yy}} + \frac{I_{zz} - I_{xx}}{I_{yy}} pr + \frac{J}{I_{yy}} p\omega_p \\
\dot{r} &= \frac{u_4}{I_{zz}} + \frac{I_{xx} - I_{yy}}{I_{zz}} pq + \frac{u_4}{I_{zz}}
\end{aligned} \tag{40}$$

where $\omega_p = \omega_1 - \omega_2 - \omega_3 + \omega_4$ is the total propeller speed.

For controller design, attitude dynamics can be linearized around hover conditions, i.e. $\phi \approx 0$, $\theta \approx 0$ and $\psi \approx 0$, where angular accelerations in body and world frames can be assumed to be approximately equal, i.e. $\dot{p} \approx \ddot{\phi}$, $\dot{q} \approx \ddot{\theta}$, $\dot{r} \approx \ddot{\psi}$. Resulting altitude and attitude dynamics can be expressed as

$$\ddot{Z} = -(c_\theta c_\phi)\frac{u_1}{m} + g,\ \ddot{\phi} = \frac{u_2}{I_{xx}},\ \ddot{\psi} = \frac{u_4}{I_{zz}},\ \ddot{\theta} = \frac{u_3}{I_{yy}} \tag{41}$$

Altitude and attitude controllers are then designed by the following expressions:

$$\begin{aligned}
u_1 &= K_{p,z} e_z + K_{d,z} \dot{e}_z + K_{i,z} \int e_z dt - \frac{mg}{c_\theta c_\phi} \\
u_2 &= K_{p,\phi} e_\phi + K_{d,\phi} \dot{e}_\phi + K_{i,\phi} \int e_\phi dt \\
u_3 &= K_{p,\theta} e_\theta + K_{d,\theta} \dot{e}_\theta + K_{i,\theta} \int e_\theta dt \\
u_4 &= K_{p,\psi} e_\psi + K_{d,\psi} \dot{e}_\psi + K_{i,\psi} \int e_\psi dt
\end{aligned} \tag{42}$$

where $e_q = q^d - q$ for $q = Z, \phi, \theta, \psi$. Note that the altitude controller given by the first equation in (42) is a gravity compensated PID controller. Similarly, other three orientation controllers are also PID controllers. In these controllers $K_{p,q} > 0$, $K_{d,q} > 0$ and $K_{i,q} > 0$ are proportional, derivative and integral control gains, respectively.

V. Simulation Results

In this section, several simulation results will be presented. Figures 3 and 4 depict the hovering and the attitude tracking performances when a disturbance observer is utilized. Thrust forces produced by the motors and the wind forces generated by the wind model are shown in Figures 5 and 6. As seen from these graphs, aerial vehicle is able to hover at a given point or in the vicinity of that despite the negative effects of the wind gusts. As can be concluded from the motion of the vehicle in the horizontal plane depicted in Figure 7, positioning errors along x and y axes did not exceed 10 cm. In addition, the vehicle's attitude angles follow reference attitude values computed by (38) and (37) very closely with an error not exceeding $\pm 2^o$. It is also obvious that during the entire flight, aerial vehicle keeps its heading and follows the reference heading angle, $\psi_{ref} = 0^o$, with an error less than 1^o.

The total disturbance estimated by the disturbance observer is plotted in Figure 8. Note that the estimated total disturbance is very similar to the dominating disturbances such as wind gusts acting on the vehicle. Successful estimation of the total disturbance on the system has a dramatic effect on the flight performance. For example, as can be seen from Figures 9 and 10 when the disturbance observer is not utilized, wind effects become dominant and position errors along x and y axes are increased a lot and large changes in the attitude of the vehicle are observed. In particular, after 80th sec wind gusts become quite dominant and dramatically affect stability of the vehicle. Therefore, the vehicle can not hover at a given point or in the vicinity of it. When the motion of the vehicle in the horizontal

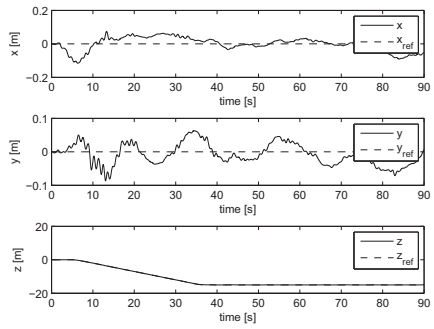

Fig. 3. Hovering performance with disturbance observer

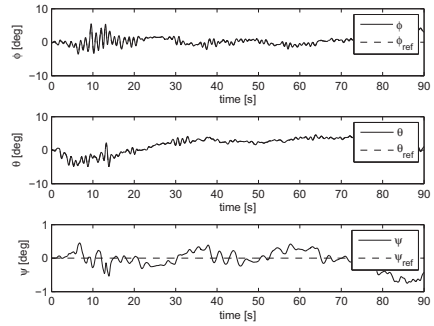

Fig. 4. Attitude performance with disturbance observer

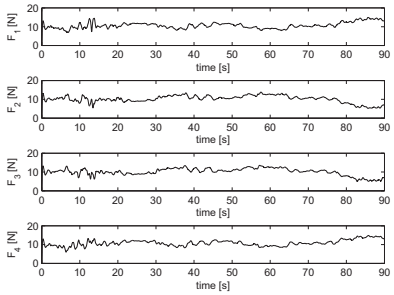

Fig. 5. Motor thrust forces with disturbance observer

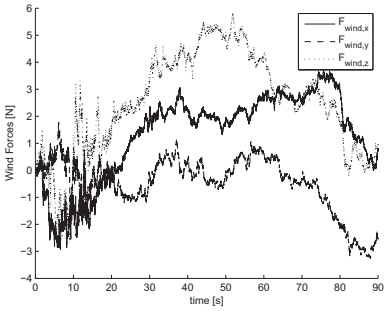

Fig. 6. Wind forces acting on the vehicle

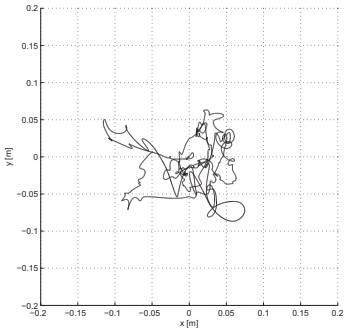

Fig. 7. Hovering performance with disturbance observer (motion in the horizontal plane)

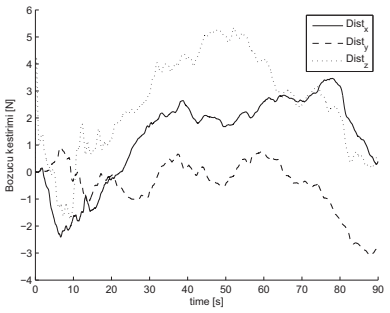

Fig. 8. Estimated total disturbance acting on the vehicle

plane depicted in Figure 11 is analyzed it is clear that the vehicle, due to disturbances, can not hover at the given point and moves away.

VI. Experimental Results

Proposed hovering controller is tested on the aerial vehicle SUAVI. Hovering controller is encoded in the onboard microcontroller and several flight tests have been performed under different weather conditions. Flight test in an open area (helicopter field) under average windy conditions is depicted in Figure 12. It is observed that actual flight performance of the vehicle is close to simulation results and the vehicle is able to hover in a robust manner. Note that the vehicle takes-off from a reference position on the ground and then keeps its position in the vicinity of that point quite successfully.

VII. Conclusion and Future Work

The proposed method in this paper has enabled a quad tilt-wing aerial vehicle to hover in the vicinity of a given point under windy conditions. Hovering performance of the vehicle is drastically improved by utilizing a disturbance observer. Designed controllers and observers are first verified with Matlab/Simulink simulations and then encoded in the onboard microcontroller. Simulation and experimental results are quite satisfactory.

As a future work, we plan to focus on the way-point tracking problem.

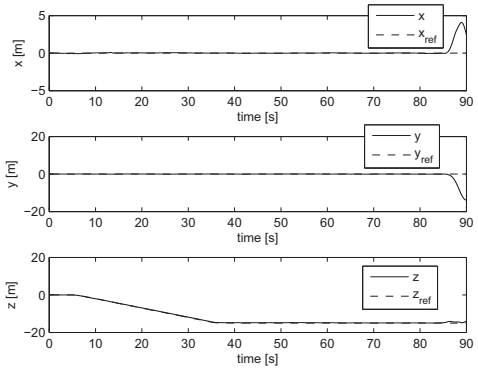

Fig. 9. Hovering performance without disturbance observer

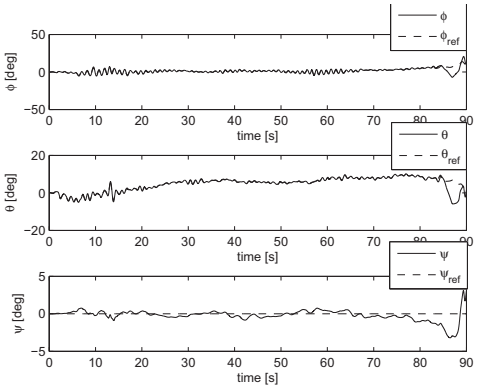

Fig. 10. Attitude performance without disturbance observer

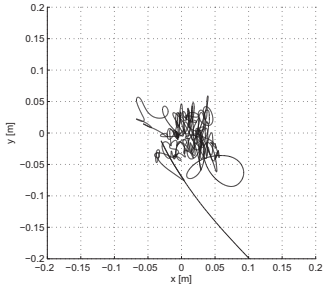

Fig. 11. Hovering performance without disturbance observer (motion in the horizontal plane)

Fig. 12. Outdoor hover test with SUAVI in helicopter field

ACKNOWLEDGMENT

Authors would like to acknowledge the support provided by TUBITAK through Grant No: 107M179.

REFERENCES

[1] Gabriel M. Hoffmann, Haomiao Huang, Steven L. Waslander, and Claire J. Tomlin, "Quadrotor helicopter flight dynamics and control: Theory and experiment", In Proceedings of the AIAA Guidance, Navigation and Control Conference and Exhibit, Hilton Head, South Carolina, August, 2007.

[2] O. Meister, R. Mnikes, J. Wendel, N. Frietsch, C. Schlaile, G. F. Trommer, "Development of a GPS/INS/MAG navigation system and waypoint navigator for a VTOL UAV", ISPIE Unmanned Systems Technology IX, Orlando, FL, USA, April 9-12, 2007, vol. 6561, p. 65611D (2007)

[3] G. M. Hoffmann, S. L Waslander, and C. J. Tomlin, "Quadrotor helicopter trajectory tracking control", In 2008 AIAA Guidance, Navigation and Control Conference and Exhibit, Honolulu, Hawaii, USA, August 2008.

[4] T. Puls, M. Kemper, R. Kke, A. Hein, "GPS Based Position Control and Waypoint Navigation System for Quadrocopters", IEEE/RSJ International Conference on Intelligent Robots and Systems, October 11-15, 2009, St. Louis, MO, USA. IEEE 2009.

[5] Steven L. Waslander and Carlos Wang, "Wind disturbance estimation and rejection for quadrotor position control", In AIAA Infotech@Aerospace Conference and AIAA Unmanned...Unlimited Conference, Seattle, WA, April 2009.

[6] S. Soundararaj, A. Sujeeth, "Autonomous Indoor Helicopter Flight Using a Single Onboard Camera", Proceedings of the IEEE International Conference on Intelligent Robots and System, St. Luis, USA, October 11-15 (2009)

[7] S. Azrad, F.Kendoul, D.Perbrianti and K. Nonami, "Visual Servoing of an Autonomous Micro Air Vehicle for Ground Object Tracking Syaril", Proceedings of the IEEE International Conference on Intelligent Robots and System, St. Luis, USA, October 11-15 (2009)

[8] K. Ohnishi, T. Murakami, "Advanced Motion Control in Robotics", IEEE, IECON, vol.2, pp.356- 359, 1989.

[9] K. T. Oner, E. Cetinsoy, E. Sirimoglu, C. Hancer, T. Ayken, M. Unel, "LQR and SMC Stabilization of a New Unmanned Aerial Vehicle", Proceedings of International Conference on Intelligent Control, Robotics, and Automation (ICICRA 2009), Venice, Italy, October 28-30, 2009.